



## Microstructure and Mechanical Properties of Surfactant Templated Nanoporous Silica Thin Films: Effect of Methylsilylation

J. Y. Chen,<sup>a</sup> F. M. Pan,<sup>b,\*</sup> A. T. Cho,<sup>b</sup> K. J. Chao,<sup>c</sup> T. G. Tsai,<sup>b</sup> B. W. Wu,<sup>b</sup>  
C. M. Yang,<sup>c</sup> and Li Chang<sup>a</sup>

<sup>a</sup>Department of Materials Science and Engineering, National Chiao Tung University, Hsinchu 30010, Taiwan

<sup>b</sup>National Nano Device Laboratories, Hsinchu 30010, Taiwan

<sup>c</sup>Department of Chemistry, National Tsinghua University, Hsinchu 30010, Taiwan

Microstructural and mechanical properties of organic surfactant templated nanoporous thin silica films have been studied by X-ray diffraction, Fourier transform infrared spectroscopy, and nanoindentation. Compared with many other porous low-*k* dielectrics, the self-assembled molecularly templated nanoporous silica films demonstrate better mechanical properties. This is ascribed to the presence of a well-ordered pore channel structure in the nanoporous silica thin films. Hardness and elastic modulus are strongly dependent on film preparation and modification methods. Trimethylsilylation by hexamethylsilazane vapor treatment effectively enhances the mechanical strength of the nanoporous silica films. When the sol precursor solution is mixed with trimethylchlorosilane (TMCS), the resulting nanoporous films have a weaker mechanical strength. The pore channel structure of the nanoporous silica film becomes less ordered for the TMCS derivatized nanoporous films. In addition, the chemical structure in the silica solid matrix of the TMCS derivatized films is more disordered than those without TMCS modification. The nanoindentation measurement results are discussed in terms of the pore microstructure of the nanoporous silica network and the springback effect due to the presence of trimethylsilyl groups in the nanopores.

© 2003 The Electrochemical Society. [DOI: 10.1149/1.1573200] All rights reserved.

Manuscript submitted October 14, 2002; revised manuscript received January 15, 2003. Available electronically April 22, 2003.

Miniaturization of integrated circuits (ICs) generally results in problems with interconnect RC delay, signal cross talk, and power consumption. In addition to the replacement of aluminum by copper to reduce interconnect resistance, interlayer dielectric (ILD) materials with an ultralow dielectric constant (*k*) are inevitably required to substitute for conventional interlayer dielectrics for sub-100 nm technology nodes. Various organic polymers,<sup>1</sup> silica sol,<sup>2-10</sup> and organic siloxanes<sup>11-13</sup> have been developed for this purpose. Among them, supported nanoporous silica thin films are considered to be the most promising materials for the sub-100 nm technology nodes because they are chemically compatible with contemporary IC processes and a *k* < 2.0 can be easily obtained owing to a high porosity. The nanoporous silica films are synthesized by either aerogel/xerogel process<sup>2-4</sup> or self-assembly molecular template method.<sup>5-10</sup> Due to the controllable porosity (45-75%) and uniform pore size distribution in the range of 2-10 nm, molecularly templated nanoporous silica films have been known to provide better mechanical and dielectric properties than aerogel/xerogel silica films. However, the mechanical strength and dielectric stability of molecularly templated nanoporous films are far inferior to that of conventional silicon oxide ILD and liable to water uptake. Before being implemented in sub-100 nm technology nodes, the nanoporous silica dielectrics need to overcome many integration challenges, such as chemical mechanical polishing (CMP) and etching.

The as-calcined nanoporous silica films are usually rich in residual silanol groups, which do not participate in the condensation reaction, and thus adsorb water molecules easily. To keep a stable dielectric property, the hydrophilic nanoporous silica films must be functionalized to achieve an acceptable hydrophobicity. Generally, this is accomplished by trimethylsilylation treatments. We have demonstrated that the hydrophobicity of a calcined silica film can be effectively improved by *in situ* trimethylchlorosilane (TMCS) silylation in the sol precursor solution, and/or a hexamethyldisilazane (HMDS) vapor post-treatment, and, with further plasma treatments, a dielectric constant less than 1.6 can be obtained.<sup>7,8</sup> However, the addition of TMCS in the sol solution may disturb the self-assembly of template molecules and hamper the condensation reaction, lead-

ing to the formation of nanoporous silica films with a less ordered pore structure and random micropores in the silica solid matrix. This makes the TMCS derivatized nanoporous films mechanically weaker.

In this work, the relation between microstructure and mechanical properties of the nanoporous silica films was studied by Fourier transform infrared spectroscopy (FTIR), X-ray diffraction spectroscopy (XRD), and nanoindentation test. Hardness and elastic modulus are strongly dependent on film preparation and modification methods. Trimethylsilylation effectively enhances the mechanical strength of the nanoporous silica films.

### Experimental

The preparation scheme for the molecularly templated silica films is shown in Fig. 1. Two sets of the nanoporous silica thin films were prepared. Both sets of nanoporous films were made from a sol solution of a mixture of tetraethyl orthosilicate (TEOS), H<sub>2</sub>O, HCl, ethanol, and a nonionic surfactant. The only difference in the preparation scheme between these two sample sets is that TMCS was added in the aged sol solution of the sample set composed of samples C and D. The template surfactant is a triblock copolymer, Pluronic P-123 (P123). The mesoporous silica films were deposited by spin coating on precleaned 4 in. p-type silicon (100) wafers. The precursor solution was prepared by adding an ethanol solution of P123 to the silica sol-gel, which was made by refluxing a mixture of TEOS, H<sub>2</sub>O, HCl, and ethanol at 70°C for 90 min. The molar ratios of reactants were 1 TEOS:0.008-0.03 P123:3.5-5 H<sub>2</sub>O:0.003-0.03 HCl:10-34 ethanol. The precursor solution was aged at room temperature for 3-6 h under ambient condition. For preparation of the TMCS derivatized nanoporous silica films, the aged sol solution was mixed with TMCS (molar ratio to TEOS 0.02-0.2) by vigorous stirring. The precursor solution was spin-coated on silicon wafers at 1600 rpm for 30 s. After spin-coating, the film was baked at 80-110°C for 1 h, followed by calcination at 350°C for 30 min in a furnace with an air flow. The resulting silica films were treated with HMDS vapor at 120°C after calcination to improve the hydrophobicity of the nanoporous films. FTIR was used to study the chemical structure of the nanoporous silica film. Surface morphology of the nanoporous films was characterized by atomic force microscopy (AFM) and scanning electron microscopy (SEM). XRD is used to study the pore microstructure of the nanoporous films. The hardness

\* Electrochemical Society Active Member.

<sup>z</sup> E-mail: fmpan@ndl.gov.tw

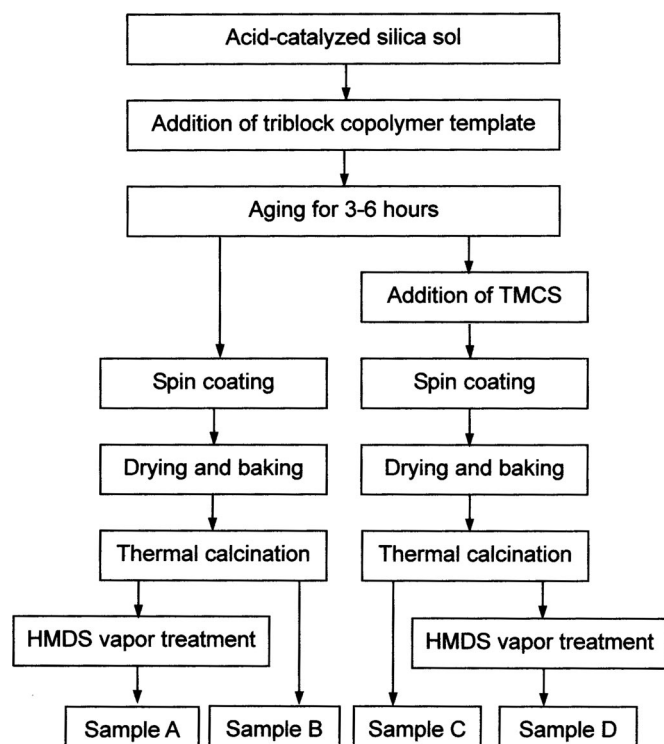


Figure 1. Sample preparation scheme for nanoporous silica thin films.

and elastic modulus of the nanoporous silica thin films were measured by a Nano Indenter XP (MTS Corp.) with a diamond tip in a Berkovich geometry. This technique allows the determination of hardness and elastic modulus depth profiles for depth down to a few tens of nanometers by progressively increasing the applied load for 0.5 to 20 mN.

### Results and Discussion

The thickness of the thin mesoporous silica films prepared as described above can be well controlled within the range of 250–450 nm, as measured by cross-sectional SEM. Figure 2 shows the cross-sectional SEM image of an as-calcined nanoporous silica thin film with no film modification. The SEM image clearly shows that the nanoporous silica thin film has a smooth surface and a uniform

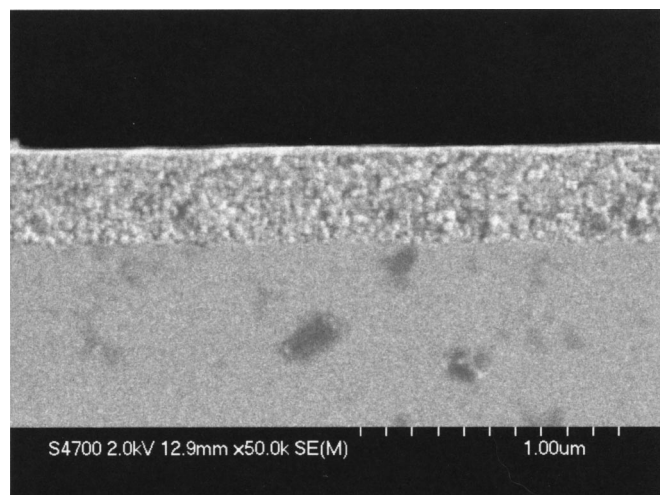


Figure 2. Cross-sectional SEM image of as-calcined nanoporous silica thin film. The film thickness is estimated to be 300 nm.

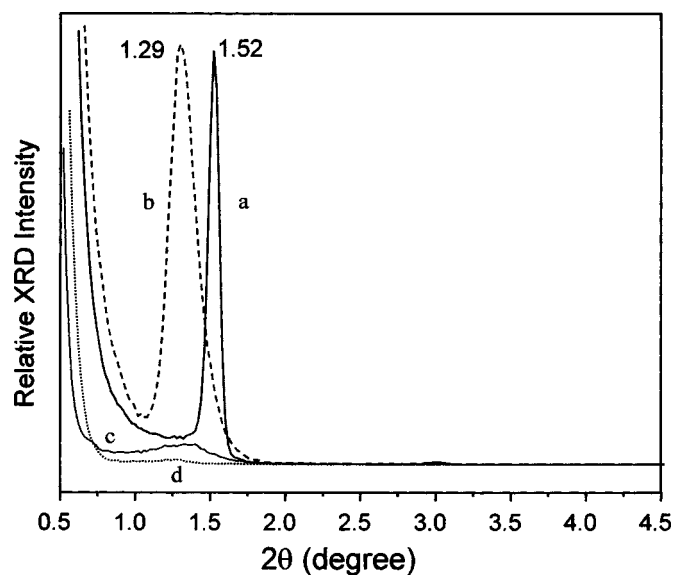
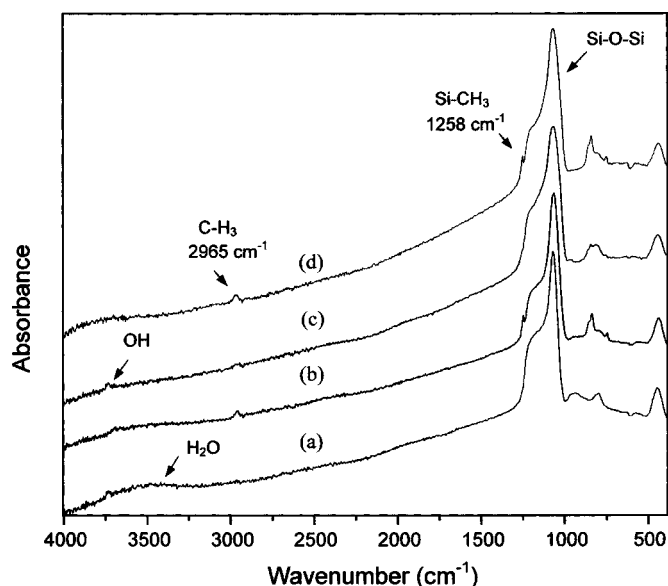


Figure 3. XRD spectra of the as-calcined nanoporous silica thin films; (a) without TMCS derivatization, (b) with 10% molar ratio TMCS, (c) with 15% TMCS, and (d) with 25% TMCS. For clarity, the XRD spectrum of the nanoporous film with 5% TMCS is not shown. The  $\langle 100 \rangle$  diffraction peak of the silica film with 5% TMCS is situated at  $2\theta = 1.42$ , and has an intensity and a fwhm comparable to the nanoporous film with 10% TMCS.

thickness. The average surface roughness was estimated to be less than 10 Å by AFM. A smooth surface and a uniform thickness are essential to an accurate nanoindentation measurement for thin-film samples. According to the krypton adsorption/desorption isotherm, the total porosity of calcined silica thin films ranges from 53 to 72% with an adjustable pore size from 43 to 80 Å, depending on the preparation of the precursor solution. Self-assembled nanoporous silica thin films templated with P123 are known to have a hexagonal pore structure.<sup>14</sup> According to the XRD spectra shown in Fig. 3, the strong  $\langle 100 \rangle$  diffraction signal reflects that the spin-coated nanoporous silica film without TMCS derivatization has an ordered pore-to-pore spacing of 61 Å after calcination. The single  $\langle 100 \rangle$  peak without any other discernible diffraction signal reveals that the pore channel array is lying parallel to the silicon substrate surface. Compared with the sample set without TMCS modification, the TMCS derivatized nanoporous silica films have a weaker and broader  $\langle 100 \rangle$  diffraction peak indicating a less ordered packing of the mesopores in the TMCS derivatized silica film. This suggests that the addition of TMCS in the sol solution significantly degrades the hexagonal pore structure of the nanoporous films. The  $\langle 100 \rangle$  diffraction peak shifts to lower diffraction angles as the TMCS concentration in the sol precursor solution increases. When the TMCS molar ratio increases from 5 to 10%, the diffraction angle  $2\theta$  shifts from 1.42 to 1.29, corresponding to an increase in the pore-to-pore spacing from 64 to 70 Å. While the pore space increases with the TMCS concentration, there is no significant difference in the intensity and the full width at half-maximum (fwhm) of the  $\langle 100 \rangle$  diffraction peaks between the 5 and 10% TMCS derivatized nanoporous films. The diffraction peak of nanoporous silica films with a TMCS molar ratio over 15%, has a  $2\theta$  angle close to that of the film with 10% TMCS, but becomes very broad and almost vanishes. The presence of TMCS in the sol precursor not only hampers condensation reactions but also perturbs self-assembly of the surfactant micelles, and thus leads to the formation of nanoporous silica thin films with a less ordered microstructure for the pore network and the silica matrix. It seems that, under the film preparation condition used in the study, there is a critical TMCS concentration in the sol precursor solution, above which the formation of an ordered self-assembled pore channel array is seriously retarded.



**Figure 4.** FTIR spectra of nanoporous silica thin films; (a) as-calcined film, (b) as-calcined film after HMDS treatment for 30 min, (c) as-calcined TMCS (10% molar ratio) derivatized film, (d) TMCS derivatized film after HMDS treatment for 30 min.

FTIR was used to study the chemical structure of the nanoporous films. Figure 4 shows the FTIR spectra of the as-deposited, HMDS treated, and TMCS derivatized nanoporous silica thin films. Compared with as-calcined nanoporous film (sample B), as-calcined TMCS derivatized sample (sample C) has a less extent of OH absorption ( $\sim 3600\text{ cm}^{-1}$ ). After treatment with HMDS vapor, both nanoporous silica thin films with and without TMCS modification are effectively trimethylsilylated as indicated by the two strong absorption peaks at  $1258$  and  $2965\text{ cm}^{-1}$ , which are due to Si-CH<sub>3</sub> and C-H<sub>3</sub> stretching vibration modes, respectively. The broad absorption band in the range of  $1080$ – $1280\text{ cm}^{-1}$  is due to asymmetric stretching of the intertetrahedral oxygen in the SiO<sub>2</sub> network, and is usually assigned to an overlap of two asymmetric stretching (AS) modes. The absorption band has been widely studied for various silica materials, and, generally, is assigned to be the overlap of two pairs of transverse optical (TO) and longitudinal optical (LO) modes.<sup>15–17</sup> Figure 5 shows that the absorption band of the as-calcined nanoporous silica film without TMCS modification can be well resolved into four peaks by curve fitting, assuming a Gaussian shape for the absorption peaks. The low wavenumber peak at  $\sim 1069\text{ cm}^{-1}$  is assigned to be a transverse optical mode (TO<sub>3</sub>), and is due to the stretching motion of oxygen atoms moving back and forth with respect to the adjacent silicon atoms and in phase with neighboring oxygen atoms. Paired with the TO<sub>3</sub> absorption is the longitudinal optical mode (LO<sub>3</sub>) centered at  $\sim 1223\text{ cm}^{-1}$ . According to previous studies, another pair of TO-LO vibration modes (denoted by TO<sub>4</sub>-LO<sub>4</sub> in the following text) is responsible for the overlapping absorption signal between the TO<sub>3</sub> and LO<sub>3</sub> peaks.<sup>15</sup> The TO<sub>4</sub>-LO<sub>4</sub> pair mode is due to the vibration in which oxygen atoms execute AS motion  $180^\circ$  out of phase with neighboring oxygen atoms. The TO<sub>4</sub> peak is estimated to center around  $1177\text{ cm}^{-1}$  and the LO<sub>4</sub> is around  $1125\text{ cm}^{-1}$  from Fig. 5. Compared with the as-calcined samples without TMCS modification, the TMCS derivatized nanoporous films have a higher absorbance for LO<sub>4</sub> and TO<sub>4</sub> vibration peaks as shown in Fig. 5.

Increasing TMCS concentration in the sol precursor results in a signal increase of the LO<sub>4</sub>-TO<sub>4</sub> pair. Kirk has shown that disorder-induced mode coupling may result in enhancement of absorption of the TO<sub>4</sub> and LO<sub>4</sub> modes.<sup>16</sup> The absorption strength of the TO<sub>4</sub> mode of bulk silica was estimated to be three to five times that of the same

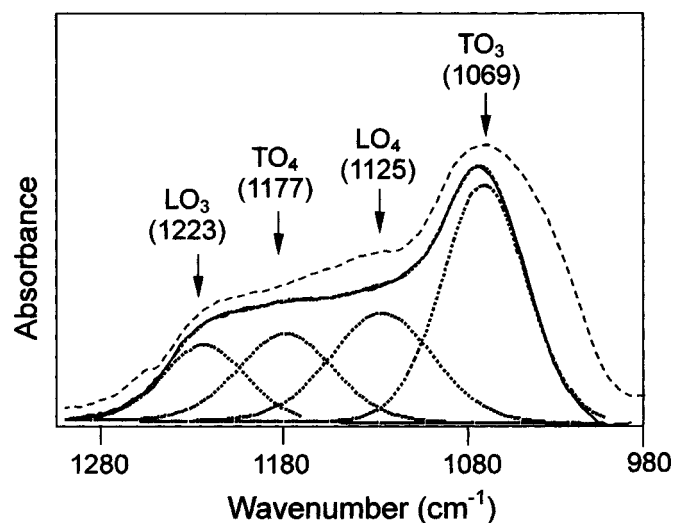


**Figure 5.** Curve fitting for the absorption band of the Si-O-Si asymmetric stretching modes of as-calcined nanoporous silica film without TMCS modification, assuming a Gaussian shape for the resolved peaks. For comparison, the absorption band of the TMCS (5%) derivatized film is also shown in the figure (dashed line). A broader and asymmetric absorption feature at the low wavenumber side can be clearly seen for the TMCS derivatized film. The broader feature is ascribed to the presence of cyclosiloxane like rings as explained in the discussion.

mode in quartz, indicating that microstructure disorder may effectively enhance the absorption strength of the out-of-phase AS mode.<sup>17</sup> Therefore, the observation of a larger absorbance of the TO<sub>4</sub>-LO<sub>4</sub> pair for TMCS derivatized nanoporous silica films suggests that the addition of TMCS in the sol solution results in a less ordered microstructure in the silica matrix of the nanoporous network. In addition, the TO<sub>3</sub> peak becomes broader and shows less symmetry at the low wavenumber side for the TMCS derivatized samples. This may be ascribed to a poorly ordered microstructure and stress effects due to the presence of terminal methyl groups inside the silica matrix.<sup>18</sup> Besides the two pairs of TO-LO modes, one more peak at the low wavenumber side ( $\sim 1030\text{ cm}^{-1}$ ) is needed to obtain a rational curve fit for the TMCS derivatized films. It is possible that random and small cyclic structures in the silica backbone, which are created due to incomplete condensation reactions and may be associated with cyclosiloxane like rings,<sup>19</sup> are responsible for the broader and asymmetric absorption band. By analyzing the intensity variation of the absorption band of the Si-O-Si stretching modes, one can determine the relative orderliness of microstructure of the silica matrix in different nanoporous silica films. The FTIR spectra in the range of  $975$ – $1300\text{ cm}^{-1}$  for the nanoporous silica thin films with and without TMCS derivatization are shown in Fig. 6. Comparison of curves c and d in Fig. 6 shows that nanoporous film with 10% TMCS has a slightly higher TO<sub>4</sub>-LO<sub>4</sub> absorption signal than the film with 5% TMCS indicating a less ordered microstructure for the former. Also shown in Fig. 6 is the absorption band of the HMDS treated nanoporous silica film (curve b). Compared with the as-calcined film (curve a), curve b shows little difference in peak shape and position except an additional peak at  $1258\text{ cm}^{-1}$  due to the Si-CH<sub>3</sub> stretching. This suggests that trimethylsilylation by the HMDS vapor treatment makes little change in the chemical structure of the silica matrix of the nanoporous films except the increase in the surface density of terminal methyl groups.

Elastic modulus is an important property characterizing the ability of porous materials to withstand stress-induced deformations. The elastic modulus and hardness of the nanoporous silica thin films are shown in Fig. 7. The TMCS derivatized nanoporous thin films have a much smaller elastic modulus and a slightly lower hardness

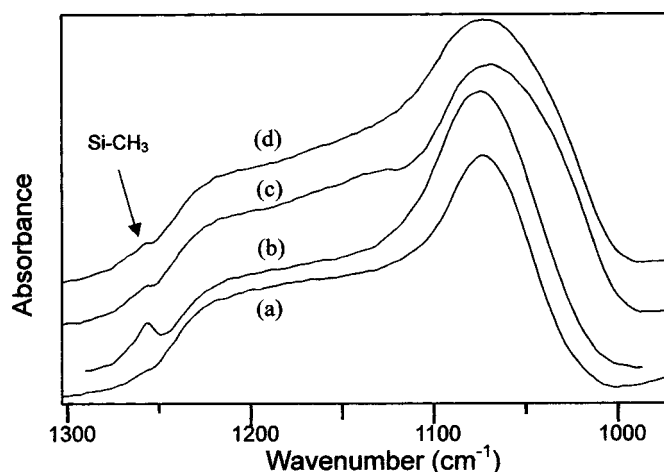


**Figure 6.** FTIR spectra of nanoporous silica thin films in the range of Si-O-Si asymmetric stretching modes; (a) as-calcined film, (b) as-calcined film after HMDS treatment for 30 min, (c) as-calcined film with 5% TMCS, (d) as-calcined film with 10% TMCS. The small peak at  $1258\text{ cm}^{-1}$  is due to the Si-CH<sub>3</sub> stretching mode.

than nanoporous films without TMCS modification. This is expected from a microstructural view point for the nanoporous thin films with an ordered pore structure. The introduction of TMCS in the precursor solution decreases the degree of the cross-linkage of the silica network and suppresses the amount of silanol groups on the silica species.<sup>9</sup> The less ordered hexagonal pore structure and a broad pore size distribution, as revealed by the XRD results, deteriorate the mechanical strength of the nanoporous films. In addition, micropores were also present in the silica matrix of the TMCS derivatized nanoporous films according to our previous study.<sup>8</sup> For porous materials, while the  $k$  value decreases linearly with increasing porosity, the mechanical properties change as a power law with density of porosity.<sup>20</sup> The presence of micropores in the silica matrix not only supplies an additional porosity to the nanoporous film leading to a lower  $k$  value, but also decreases the density of the silica matrix. The molecularly templated nanoporous silica thin films prepared in this work can be considered as cellular material with a thick cell

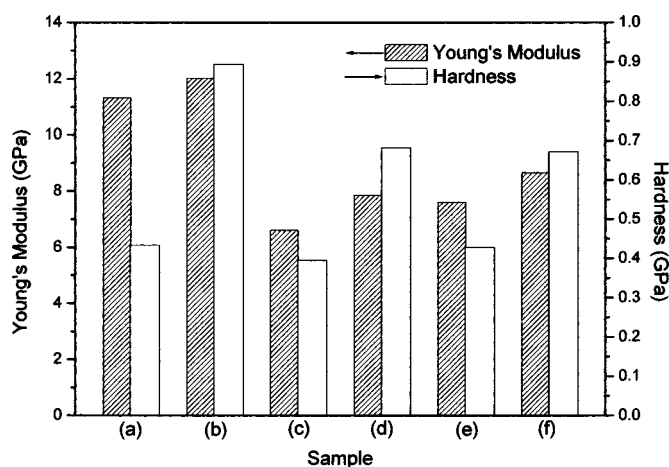


**Figure 7.** Young's modulus and hardness of nanoporous silica thin films; (a) as-calcined film, (b) as-calcined film after HMDS treatment for 30 min, (c) as-calcined TMCS (5% molar ratio) derivatized film, (d) TMCS (5% molar ratio) derivatized film after HMDS treatment for 30 min, (e) as-calcined TMCS (10% molar ratio) derivatized film, (f) TMCS (10% molar ratio) derivatized film after HMDS treatment for 30 min.

wall. For cellular materials, a reduction in the density of the cell wall certainly decreases the elastic modulus and other mechanical properties.<sup>21</sup>

Nanoindentation measurements show that the mechanical strength of the nanoporous films can be greatly improved by trimethylsilylation. As shown in Fig. 7, the nanoporous silica films, both with and without TMCS derivatization, gain an increase in hardness by a factor of more than 75% after HMDS vapor treatment for 30 min. An increase of <20% in Young's modulus was observed. The improvement of mechanical strength can be attributed to the presence of trimethylsilyl groups on the pore surfaces. The mechanical strength of the 5% TMCS derivatized nanoporous film is somewhat weaker than that of the 10% TMCS derivatized film. As discussed previously, a higher TMCS content in the sol-gel precursor solution leads to the formation of a less ordered nanoporous silica network, resulting in weaker mechanical strength. The observation of the opposite trend is ascribed to that more terminal trimethylsilyl groups in the 10% TMCS derivatized film may enhance the mechanical strength due to a springback effect, and thereby compensate for the loss of the mechanical strength caused by the less ordered structure. Prakash *et al.*<sup>22</sup> and Smith *et al.*<sup>20</sup> have reported a "springback" feature for aerogel and xerogel films during the drying stage. The thickness of the xerogel film or the volume of the silica gel which receives methylation treatments can recover to a certain extent after the gel reaches its greatest compaction. On the contrary, shrinkage of the gel is completely irreversible for those nonmodified nanoporous silica thin films. The springback feature is attributed to the presence of terminal organosilane groups that cannot participate in condensation reactions. The electrostatic repulsion interaction between the crowded and bulky trimethylsilane groups on pore surfaces may effectively increase the resistance of the silica network to deformation under an applied load.

## Conclusion

Microstructural and mechanical properties of organic surfactant templated nanoporous thin silica films have been studied by XRD, FTIR, and nanoindentation. Compared with many other porous low- $k$  dielectrics, the self-assembled molecularly templated nanoporous silica films demonstrate better mechanical properties. This is ascribed to the presence of a well-ordered pore channel structure in the nanoporous silica films. When the sol precursor solution is mixed with TMCS, the resulting nanoporous films have a weaker mechanical strength. The pore channel structure of the nanoporous silica film becomes less ordered for the TMCS derivatized nanoporous films. In addition, FTIR analysis reveals that the chemical structure in the solid matrix of the porous network of the TMCS derivatized films is more disordered than those without TMCS modification. Trimethylsilylation by the HMDS vapor treatment can significantly improve the mechanical strength of the nanoporous silica thin films. The nanoindentation measurement results can be explained in terms of the pore microstructure of the nanoporous silica network and the springback effect due to the presence of trimethylsilyl groups in the nanopores.

## Acknowledgments

This work was supported by the National Science Council of the Republic of China under the contract no. NSC90-2722-2317-200 and NSC90-2215-E317-003. Technical support from the National Nano Device Laboratories is gratefully acknowledged.

National Nano Device Laboratories assisted in meeting the publication costs of this article.

## References

- S. J. Martin, J. P. Godschalx, M. E. Mills, E. O. Shaffer II, and P. H. Townsend, *Adv. Mater.*, **12**, 1769 (2000).
- M. H. Jo, H. H. Park, D. J. Kim, S. H. Hyun, S. Y. Choi, and J. T. Paik, *J. Appl. Phys.*, **82**, 1299 (1997).
- J. H. Kim, S. B. Jung, H. H. Park, and S. H. Hyun, *Thin Solid Films*, **377**, 467 (2000).

4. S. V. Nitta, A. Jain, P. C. Wayner, Jr., W. N. Gill, and J. L. Plawsky, *J. Appl. Phys.*, **86**, 5870 (1999).
5. D. Zhao, P. Yang, N. Melosh, J. Feng, B. F. Chmelka, and G. D. Stucky, *Adv. Mater.*, **10**, 1380 (1998).
6. S. Baskaran, J. Liu, K. Domansky, N. Kohler, X. Li, C. Coyle, G. E. Fryxell, S. Thevuthasan, and R. E. Williford, *Adv. Mater.*, **12**, 291 (2000).
7. A. T. Cho, T. G. Tsai, C. M. Yang, K. J. Chao, and F. M. Pan, *Electrochem. Solid-State Lett.*, **4**, G35 (2001).
8. C. M. Yang, A. T. Cho, F. M. Pan, T. G. Tsai, and K. J. Chao, *Adv. Mater.*, **13**, 1099 (2001).
9. T. G. Tsai, A. T. Cho, C. M. Yang, F. M. Pan, and K. J. Chao, *J. Electrochem. Soc.*, **149**, F116 (2002).
10. S. Pevzner, O. Regev, and R. Yerushalmi-Rozen, *Curr. Opin. Colloid Interface Sci.*, **4**, 420 (2000).
11. T. C. Chung, P. T. Liu, Y. S. Mor, S. M. Sze, Y. L. Yang, M. S. Feng, F. M. Pan, B. T. Dai, and C. Y. Chang, *J. Electrochem. Soc.*, **146**, 3802 (1999).
12. D. G. Shamiryan, M. R. Baklanov, S. Vanhaelemeersch, and K. Maex, *Electrochem. Solid-State Lett.*, **4**, F3 (2001).
13. A. Grill and V. Patel, *Appl. Phys. Lett.*, **79**, 803 (2001).
14. D. Zhao, Q. Huo, J. Feng, B. F. Chmelka, and G. D. Stucky, *J. Am. Chem. Soc.*, **120**, 6024 (1998).
15. C. Vautey, M. Burgos, and M. Langlet, *Thin Solid Films*, **347**, 184 (1999).
16. C. T. Kirk, *Phys. Rev. B*, **38**, 1255 (1988).
17. P. H. Gaskell and D. W. Johnson, *J. Non-Cryst. Solids*, **20**, 171 (1976).
18. N. Primeau, C. Vautey, and M. Langlet, *Thin Solid Films*, **310**, 47 (1997).
19. H. G. P. Lewis, T. B. Casserly, and K. K. Gleason, *J. Electrochem. Soc.*, **148**, F212 (2001).
20. D. M. Smith, D. Stein, J. M. Anderson, and W. Ackerman, *J. Non-Cryst. Solids*, **186**, 104 (1995).
21. X. E. Guo and L. J. Gibson, *Int. J. Mech. Sci.*, **41**, 85 (1999).
22. S. S. Prakash, C. J. Brinker, and A. J. Hurd, *J. Non-Cryst. Solids*, **190**, 264 (1995).